

**Multi-walled/Single-walled Carbon
Nanotube (MWCNT/SWCNT) Interconnect
Lumped Compact Model Considering Defects,
Contact resistance and Doping impact
v.1.0.0**

Contributing authors:

CNRS-LIRMM/University of Montpellier

Dr. Rongmei Chen, email: Rongmei.chen@lirmm.fr

Ph.D student: Jie Liang, email: Jie.liang@lirmm.fr

Dr. Aida Todri-Sanial, email: Aida.todri@lirmm.fr

Device Modelling Group, University of Glasgow

Dr. Jaehyun Lee, email: Jaehyun.Lee@glasgow.ac.uk

Dr. Vihar Georgiev, email: Vihar.Georgiev@glasgow.ac.uk

All rights reserved.

July 11, 2018

Content

I. Introduction.....	3
II. Compact model descriptions.....	3
1. Pristine MWCNT/SWCNT	3
2. Doped MWCNT	5
3. Variability study.....	6
A. Diameter variation.....	6
B. Defect resistance variation.....	6
C. Chirality variation.....	6
III. Parameters setup	6
IV. Simulation setup and results	7
1. Simulation setup.....	7
2. Simulation results with template parameters	8
D. Delay/power/PDP change with diameters of MWCNT/SWCNT	8
E. Delay with Fermi level shift of MWCNT/SWCNT.....	9
F. Delay with defect density in each shell of MWCNT or SWCNT.....	9
G. Delay with chirality of MWCNT/SWCNT	9
H. Monte Carlo simulation for MWCNT and SWCNT	10
V. References.....	11

I. Introduction

Currently, CNT is considered as one of the primary candidates to outperform Cu concerning performance and reliability as future back-end-of-line (BEOL) interconnect material due to its properties such as ballistic transport, high thermal conductivity, ampacity and strong sp_2 bonding between carbon atoms.

Good contacts between CNT and metal electrodes are very challenging. Poor contacts generate significant contact resistance, which severely degrades the performance of CNT as interconnects. Basically, there are two kinds of contacts such as side-contact and end-contact. The side-contact relies on Van der Waals bond while the end-contact has covalent metal-carbon bonds as an interface. In this manual, we use and describe the end-contact. The selected metal electrode is Pd. It should be noted that SWCNT is a particular case of MWCNT and so in the following introduction and discussion, MWCNT is regarded as a representative of CNT interconnect.

On CVD grown CNTs, defects are omnipresent and may impact its performance. The most typical types include vacancies, interstitials, non-hexagonal rings and grain boundaries [1]. Defects can trap or scatter carriers and thus, ultimately impact CNT interconnect performance. Furthermore, CNT diameter, chirality, and defect variations are found to play an essential role in determining the CNT performance as interconnects. So, a MWCNT/SWCNT compact model capable of evaluating the impact of the defects, diameter and chirality variations on its performance is of high interest.

In this project, we present SWCNT and MWCNT interconnect compact models. These models consider the impact of CNT defects, the chirality and contact resistance between CNT-electrode (Pd) on CNT interconnect performances and power consumption. Variabilities of diameter, defect resistance and chirality are also considered in these models by enabling Monte Carlo simulation. Furthermore, the increase in charge based doping of CNT with $PtCl_4$ is evaluated by Fermi level shift which changes the conducting channel of CNT and then impact the performance, power consumption and variability of CNT interconnect.

II. Compact model descriptions

1. Pristine MWCNT/SWCNT

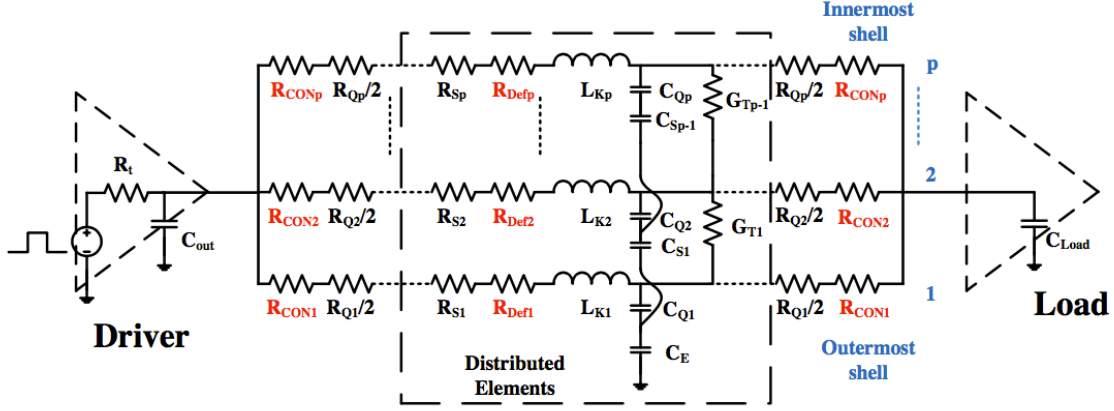


Fig. 1. Proposed advanced distributed compact model of MWCNT. SWCNT can be obtained by connecting only the outermost shell of MWCNT to the electrodes (namely a particular case of MWCNT) and is thus not discussed in addition.

The proposed advanced compact model of MWCNT as shown in Fig. 1 is based on the original well known compact model developed by [2]. Except the contact resistance R_{CON} and defects induced resistance R_{Def} , all parameters are calculated similarly to those in [2]. The number of shells for a MWCNT is calculated based on Equations (1) and (2) as shown below. The p refers to the number of shells in the MWCNT. D_{CNTmax} represents the outermost or largest diameter of the MWCNT. d is the van der Waals gap and equals to 0.34 nm. D_{CNTi} is the diameter of the i^{th} shell ($i=(1, p)$, 1 represents the outermost shell and p the innermost shell) in the MWCNT.

$$p = 1 + \text{Inter} \left[\frac{(D_{CNTmax} - D_{CNTmax}/2)}{2d} \right] \quad (1)$$

$$D_{CNTi} = D_{CNTmax} - 2d(i - 1), \quad 1 \leq i \leq p \quad (2)$$

The intrinsic resistance of CNT shells can be calculated by Equations (3) and (4) where R_Q , N_C and λ_i represent quantum resistance, the number of conducting channels, which can be calculated by an analytical method as will be introduced in the following doped MWCNT part, and mean free path (MFP) of the CNT shell i respectively. $h/2e^2 \sim 12.9 \text{ k}\Omega$ and L is the CNT shell length.

$$R_i = R_Q + R_{Si}L = \frac{h}{2e^2 N_{Ci}} + \frac{h}{2e^2 N_{Ci}} \frac{L}{\lambda_i} \quad (3)$$

$$\lambda_i \approx 1000 D_{CNTi} \quad (4)$$

In [3], atomistic-level simulations showed that vacancy-type defects induced resistance $R_{DEFi}(\Omega)$ in metallic CNTs is proportional to the defect density N_{Defi} (/nm) and is inversely dependent on the shell diameter D_{CNTi} (Å) as shown in Equation (5), where L is the CNT shell length. This defect-induced resistance is distributed uniformly along each MWCNT shell as shown in Fig. 1. Furthermore, the density of defect vacancies is assumed to be not dependent on the diameter of each shell. As a result, N_{Defi} is the same

for each shell and the difference of R_{DEFi} between shells results from their diameter difference.

$$R_{DEF}(N_{Def_i}, D_{CNT_i})_i = 2.67 \times 10^5 \times N_{Def_i} \times L \times D_{CNT_i}^{-1.27} \quad (5)$$

The Pd-CNT (for each shell) contact resistance can be indirectly obtained by atomistic level simulation results of end-contact of Pd-SWCNT (as shown in Equation (6)) and regarding each shell of MWCNT as a SWCNT of various diameters.

$$R_{CON_i} = 1.8514A_i^{-1} + 1.4685 \quad (\text{k}\Omega) \quad A_i = \frac{\pi D_{CNT_i}^2}{4} \quad (6)$$

Based on the advanced distributed compact model in Fig. 1, a corresponding lumped compact model is shown in Fig. 2. The lumped parameters are calculated by multiplying the distributed parameters with the length of MWCNT. It has been demonstrated by simulation that for MWCNT local interconnect applications, the lumped compact model is accurate and much more efficient than the distributed compact model.

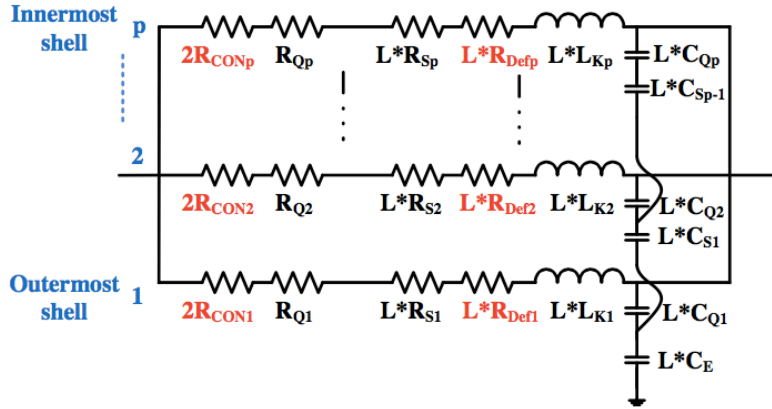


Fig. 2. Proposed advanced lumped compact model

2. Doped MWCNT

Here, we present an analytical method for computing the impact of doping on the number of conducting channels N_C via the Fermi level shift E_f . The band structure of a zigzag CNT with chirality of $(m, 0)$ can be described by Equation (7) [4], where D_{CNT} is the CNT diameter, k_x is the wave vector in the x direction, t is the hopping parameter, a_0 is the carbon-carbon distance, and ν is an integer less than m (can be calculated from D_{CNT} [4]). E_f is assumed to be 0.0 eV for pristine zigzag CNT. From Equation (7), we can calculate the transmission coefficients ($T(E)$), and then the number of conducting channel N_C can be obtained as shown in Equation (8) [4]. It should be noted that the N_C of metallic armchair CNT can be calculated similarly [6]. In this way, the intrinsic resistance of each shell of CNT in MWCNT can be calculated (in Equation (3)) and thus the whole resistance of MWCNT as illustrated in Fig. 1.

$$E(k_x) = \pm \frac{3ta_0}{2} \sqrt{k_x^2 + \left(\frac{1}{D_{CNT}} (2v - \frac{4}{3}m) \right)^2} \quad (7)$$

$$N_C = \int T(E) f'(E, E_f) dE / (k_B T) \quad (8)$$

3. Variability study

Diameter variation

It is assumed that the diameter variation on MWCNT is evaluated by the outermost diameter of MWCNT, namely D_{max} , which has a Gaussian distribution. For example, D_{max} complies with a Gaussian distribution with the $\sigma_{D_{max}}$ varying 15% of the $\mu_{D_{max}}$, namely $N(\mu_{D_{max}}, (15\% \times \mu_{D_{max}})^2)$.

Defect resistance variation

We assume that defect-induced resistance R_{Def} is a Lognormal distribution with $\ln(R_{Def}) \sim N(\mu_{LogN}, (\mu_{LogN} \times 0.0497)^2)$ μ_{LogN} can be calculated based on the mean of R_{Def} as shown in the Equation (5) aforementioned [7].

Chirality variation

The chirality of each shell in a MWCNT is assumed to be independent and comply with Bernoulli distribution (or 0-1 distribution) with each shell of 1/3 (or 2/3) probability to be metallic (or semiconducting).

III. Parameters setup

There are two Verilog-A models for CNT interconnect. One is for normal simulation and the other is for Monte Carlo simulation as their file names specified.

User-defined input parameters for the lumped compact model are introduced in the Table I.

Table I. User-defined input parameters to the lumped compact model

Name	Suggested Scope	Description
L	(0, 20um]	Length of MWCNT
H	1 um	Distance between MWCNT and ground
Chi	(0,1]	Default chirality of MWCNT or portion of metallic shells in MWCNT
Def	[0, inf)	Defect density (/nm)
k	[0, p), p is the number of shells for a MWCNT	the 1~k shells of MWCNT are broken (from the outermost to the inner shell)
j	[0, p), p is the number of shells for a MWCNT	the 1~j shells of MWCNT are broken (from the innermost to the outer shell)
Mo	0 or 1	Chirality variation on (for Monte

		Carlo simulation) or off (for normal simulation), 1:on; 0:off
$Defo$	0 or 1	Defect variation on (for Monte Carlo simulation) or off (for normal simulation), 1:on; 0:off
D_{max}	(0, 20 nm]	Outermost diameter of the MWCNT
E_f	[0, inf)	Fermi level shift
MS	0 or 1	Selection of MWCNT or SWCNT, 0:SWCNT (diameter is D_{max}), 1:MWCNT
$Rcdefine$	0 or 1	Selection of electrode-MWCNT contact resistance R_c calculation methods, 0: R_c is calculated automatically in the model, which is based on Pd-CNT atomistical level simulation results and empirical extrapolation; 1: user input R_c values
R_c	Not limit	User input contact resistance value

IV. Simulation setup and results

1. Simulation setup

For normal simulation, the parameters in the Table I can be set properly and proceed with simulation. If Monte Carlo simulation is desired, the input parameters need to be set differently such as by assuming some kinds of distributions to some interested parameters. Here we assume that Cadence spectre tool is used for Monte Carlo simulation and the corresponding setup is introduced. A library file needs to be created with name MCmodel.scs which is further included into the library model of a simulation.

For the simulation of MWCNT-interconnect performance, including delay, power and power delay product (PDP), the schematic shown in Fig. 3 is used. MWCNT lumped compact model is used to represent interconnect between inverters composed of CNFET (Stanford university model [8], with default parameters in the manual used). The supply voltage is 0.7 V and the rise and fall times of input square wave are both 5 ps.

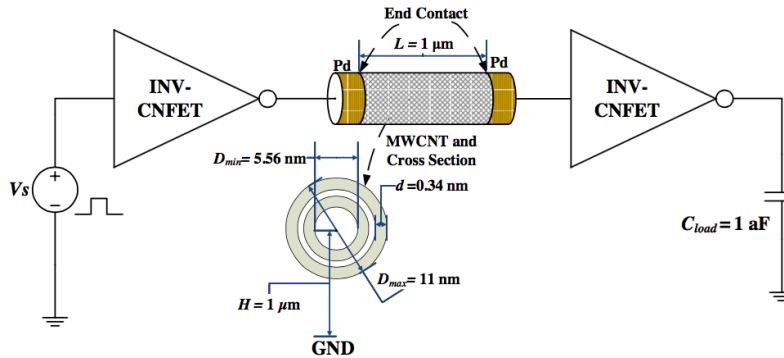


Fig. 3. Simulation setup schematic

2. Simulation results with template parameters

Table II. User-defined input parameters for a case study

Input	Default value without specification
L	1 μm
H	1 μm
Chi	1/3
Def	10
k	0
j	0
Mo	0
$Defo$	0
$Dmax$	11 nm
Ef	0
MS	1 and 0 for MWCNT and SWCNT respectively
$Rcdefine$	0
Rc	0

A. Delay with the diameter of MWCNT/SWCNT

As shown in Fig. 4, the delay of MWCNT/SWCNT interconnect with the parameters listed in the Table II are all decreased significantly as the diameter increases. Compared with SWCNT of the same diameter, the MWCNT interconnects have much better performances.

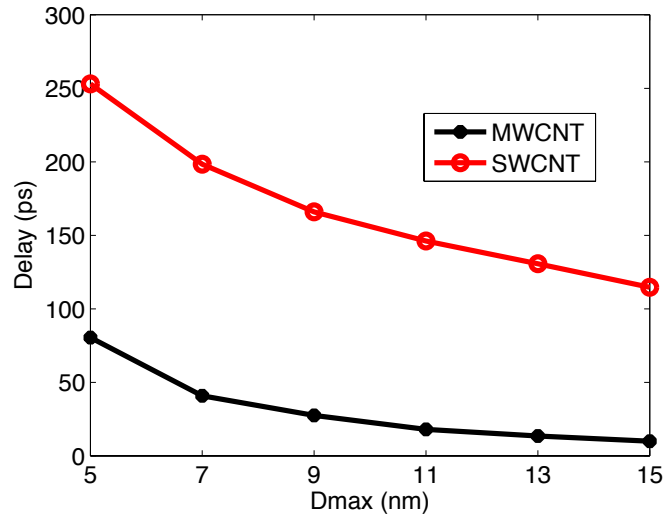


Fig. 4. Delay changes with the diameter of MWCTN/SWCNT

B. Delay with Fermi level shift of MWCNT/SWCNT

It is clearly shown in Fig. 5 that as the Fermi level of MWCNT/SWCNT is shifted by doping, the delay of both MWCNT and SWCNT is significantly reduced, especially at the first stage of Fermi level shift. After Fermi level is shifted significantly such as up to 0.2 eV, only slightly furthermore improvement of performance is observed due to the more and more dominant impact from contact and defect resistances.

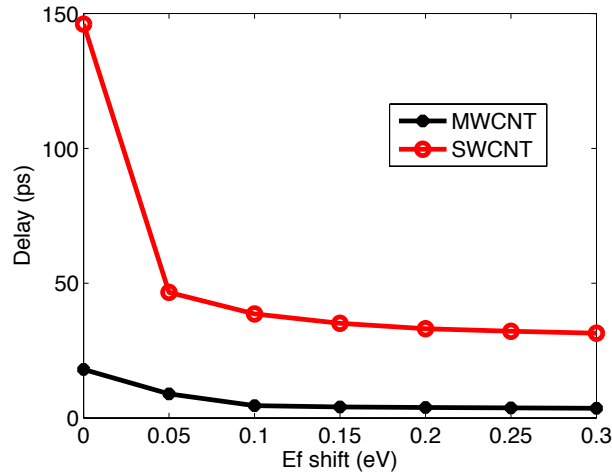


Fig. 5. Delay changes with Fermi level shift of MWCNT/SWCNT by doping

C. Delay with defect density in each shell of MWCNT or SWCNT

As shown in Fig. 6, the delay of both MWCNT and SWCNT is increased with defect density in shells of MWCNT or SWCNT.

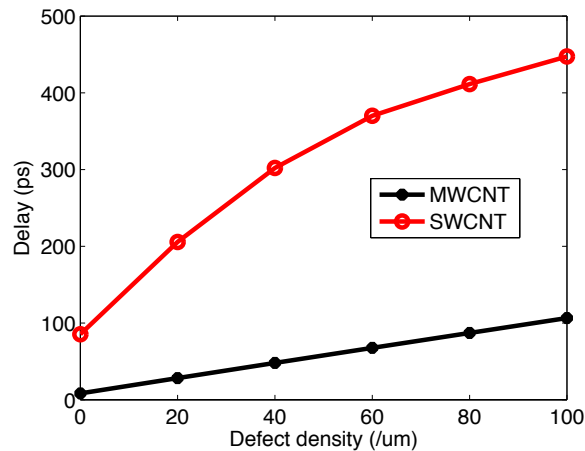


Fig. 6. Delay changes with defect density of MWCNT/SWCNT by doping

D. Delay with chirality of MWCNT/SWCNT

As the chirality of MWCNT/SWCNT or the portion of metallic CNT is improved, the delay of both MWCNT and SWCNT are reduced significantly. Nearly 70% of delay improvement is observed for both of them when chirality is changed from 1/3 (without any chirality optimization during fabrication) to 1 (total metallic CNT).

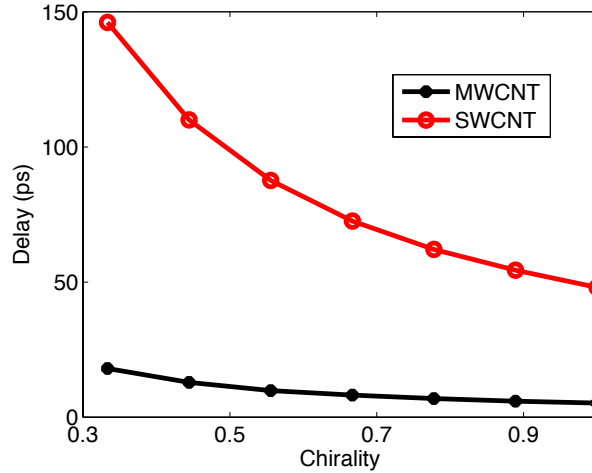


Fig. 7. Delay changes with chirality of MWCTN/SWCNT by doping

E. Monte Carlo simulation for MWCNT

Here we present variability study of diameter (Dmax), defects, chirality and all-sources variations by performing MC simulations for them. The all-sources variation refers to the case that diameter, defects and chirality variations are simultaneously considered. The diameter, defect and chirality variations are randomized respectively as follows: D_{CNTmax} (Gaussian distribution $N(11 \text{ nm}, 1.65^2 \text{ nm})$), R_{Def} (LogN distribution, $\ln(R_{Def}) \sim N(\mu_{LogN}, (\mu_{LogN} \times 0.0497)^2)$, μ_{LogN} can be calculated based on the mean of R_{Def} in Equation (5)), and each CNT shell chirality (0-1 distribution, 1/3 to be metallic). The all-sources variation has the above all parameters randomized simultaneously. Delay of MWCNT interconnect (except the randomized parameters, other parameters are the same to Table II) variations as a result of these variations are shown in Fig. 8 – Fig.11 respectively.

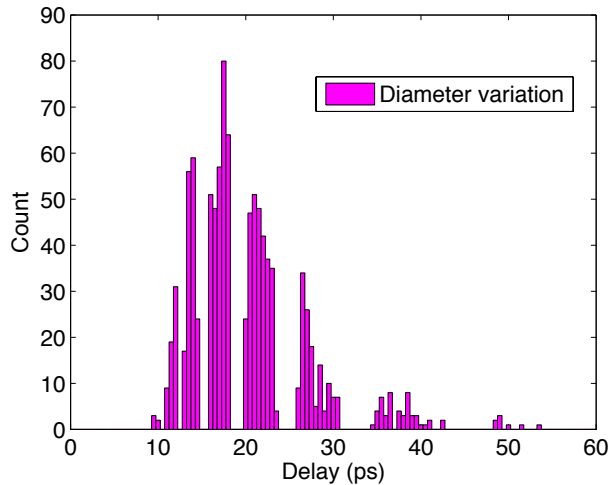


Fig. 8. Diameter variation results. The mean and standard deviation of delay is 20.2 ps and 6.7 ps respectively.

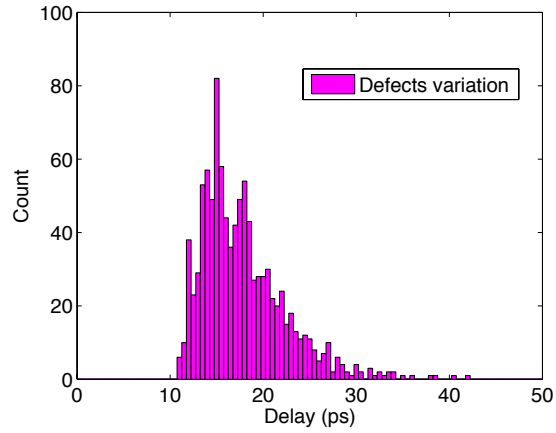


Fig. 9. Defects variation results. The mean and standard deviation of delay is 17.8 ps and 4.6 ps respectively.

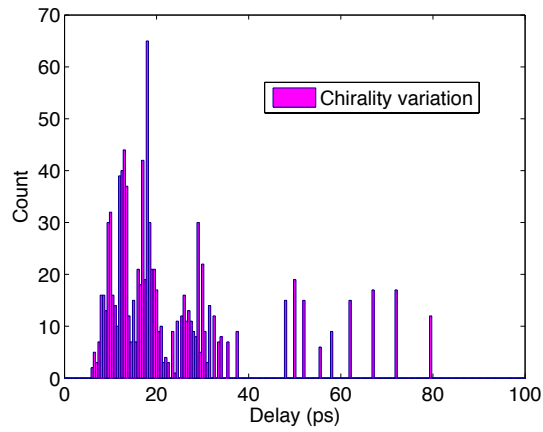


Fig. 10. Diameter variation results. The mean and standard deviation of delay is 23.5 ps and 16.0 ps respectively.

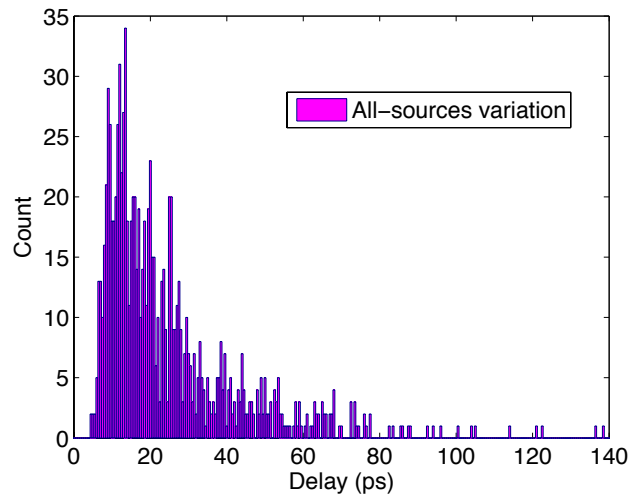


Fig. 11. Diameter variation results. The mean and standard deviation of delay is 24.7 ps and 18.5 ps respectively.

V. References

- [1] P. G. Collins, "Defects and disorder in carbon nanotubes," in *Oxford Handbook of Nanoscience and Technology Volume 2: Materials: Structures, Properties and Characterization Techniques*. Oxford University Press Oxford, 2009, pp. 156–184.
- [2] H. Li, W.-Y. Yin, K. Banerjee, and J.-F. Mao, "Circuit modeling and performance analysis of multi-walled carbon nanotube interconnects," *IEEE Transactions on electron devices*, vol. 55, no. 6, pp. 1328–1337, 2008.
- [3] J. Lee, S. Berrada, J. Liang, T. Sadi, V. P. Georgiev, A. Todri-Sanial, D. Kalita, R. Ramos, H. Okuno, J. Dijon *et al.*, "The impact of vacancy defects on cnt interconnects: From statistical atomistic study to circuit simulations," in *Simulation of Semiconductor Processes and Devices (SISPAD), 2017 International Conference on*. IEEE, 2017, pp. 157– 160.
- [4] H. H. B. Sørensen, P. C. Hansen, D. E. Petersen, S. Skelboe, and K. Stokbro, "Efficient wave-function matching approach for quantum transport calculations," *Physical Review B*, vol. 79, no. 20, p. 205322, 2009.
- [5] Wong, H-S. Philip, and Deji Akinwande. *Carbon nanotube and graphene device physics*. Cambridge University Press, 2011.
- [6] S. Datta, *Quantum transport: atom to transistor*. Cambridge university press, 2005.
- [7] P. Holgate, "The lognormal characteristic function," *Communications in Statistics-Theory and Methods*, vol. 18, no. 12, pp. 4539–4548, 1989.
- [8] C.-S. Lee, E. Pop, A. D. Franklin, W. Haensch, and H.-S. Wong, "A compact virtual-source model for carbon nanotube fet's in the sub-10-nm regime part i: Intrinsic elements," *IEEE transactions on electron devices*, vol. 62, no. 9, pp. 3061–3069, 2015.